RECENT RESULTS OF H-MODE STUDIES ON ASDEX

F. WAGNER, F. RYTER, A.R. FIELD, G. FUSSMANN, J.V. HOFMANN, M.E. MANSO[1], O. VOLLMER, R. BÜCHSE, G. DODEL[2], A. EBERHAGEN, M. ENDLER, W. ENGELHARDT, H.-U. FAHRBACH, O. GEHRE, J. GERNHARDT, L. GIANNONE, O. GRUBER, H.J. HARTFUSS, W. HERMANN, E. HOLZHAUER[2], A. KALLENBACH, O. KARDAUN, F. KARGER, O. KLÜBER, M. KORNHERR, K. LACKNER, R. LANG, J. MATIAS[1], H.-M. MAYER, K. McCORMICK, V. MERTENS, E.R. MÜLLER, H.D. MURMANN, J. NEUHAUSER, H. NIEDERMEYER, W. POSCHENRIEDER, A. RUDYJ, U. SCHNEIDER, R. SCHUBERT, G. SILLER, E. SIMMET, F.X. SÖLDNER, A. STÄBLER, K.-H. STEUER, U. STROTH, N. TSOIS[3], H. VERBEEK, H. ZOHM
Max-Planck-Institut für Plasmaphysik,
Euratom–IPP Association,
Garching, Federal Republic of Germany

Abstract

RECENT RESULTS OF H-MODE STUDIES ON ASDEX.

In a comparative study of various confinement regimes the H-mode demonstrated the best performance. Confinement enhancement factors (above ITER 89-P L-mode scaling) in the range of $1.6 \leq f_H \leq 2.8$ have been achieved with values depending on the divertor configuration, the wall condition, ELM behaviour and the plasma ion species. Long-pulse H-phases, with ELMs, of up to 3.5 s with constant confinement time, recycling and impurity characteristics are achieved. H*-mode operation is possible without a loss of current scaling at q_a values as low as 2.2. The β-limit is the same with and without ELMs. Murakami parameters are similar in H- and L-modes ($M \leq 10 \times 10^{19}$ $m^{-2} \cdot T^{-1}$). A high perpendicular edge rotation velocity $v_\perp$ is observed in the H-phase. $v_\perp$ develops gradually during the H-phase and increases with NI power. Though edge turbulence drops initially after the H-transition, edge fluctuations appear again in quiescent phases which reduce the edge electron temperature. An ELM precursor has been identified in the frequency range of $100 \leq f \leq 200$ kHz. ELM induced losses set in during an turbulent phase following the precursor. ELM characteristics are the same at low or high edge pressure, for singular or 'grassy' ELMs.

---

[1] Instituto Superior Tecnico, Lisbon, Portugal.
[2] Universität Stuttgart, Federal Republic of Germany.
[3] National Research Centre for the Physical Sciences Democritos, Athens, Greece.

1 INTRODUCTION

On ASDEX we have developed a sequence of confinement regimes in order to explore their inherent transport physics and also, to assess their performance:

(1) Degraded confinement regimes with medium peaked density profiles { Saturated Ohmic Confinement [SOC], L-mode (co-NI)},

(2) Improved confinement regimes with peaked density profiles { Improved Ohmic Confinement [IOC], pellet refuelled discharges [PD], L-mode counter neutral injection [ctr-NI] } [1],

(3) H-mode with flat density profiles [2].

SOC and IOC are obtained under ohmic conditions (OH), L-mode co and ctr, and H-mode with NI, and PD both under OH and NI conditions. All improved regimes are distinguished by a substantial rise in the confinement time ($\geq$ 50%). Transport analysis has benefitted from the possibility to compare regimes: SOC and IOC, L-mode (co-NI) and either H-mode or ctr-NI, gas-puff and pellet refuelling. The peaking of the density profile preferentially reduces the ion transport [1]; the edge transport barrier of the H-mode, first described in [3], leads to a substantial reduction of the electron transport. Momentum balance analysis of plasma rotation played a decisive role in the identification of the loss channel which causes the difference between an improved and a degraded regime [1].

The peaked density regimes have the following disadvantages: The IOC regime is limited to low power fluxes across the separatrix [5]. Higher power fluxes lead to the SOC or the L-regime. Ctr-NI plasmas with improved confinement never reached steady state and always disrupted. PD show a strong degradation of confinement with auxiliary heating power toward the usual L-mode level [1]. Both with ctr-NI [6] and in the quiescent phases of PD impurities accumulate with approximately neo-classical rates.

This comparative study showed that the best performance, the largest operational range, and the best prospects for satisfying the various reactor requirements can be expected from the H - mode. In the following, we will discuss the progress we made in H-mode studies.

2 CONSTRAINTS ON THE DIVERTOR CONFIGURATION FOR GOOD H-MODES

The major requirements for access to the H-mode at low power - divertor configuration and ion-drift to the X-point [7] - are well documented. The importance of recycling [8] and impurity control will be addressed here.

Tab. 1. Exponents of the regression analysis in the form τ_E (ms) = const × $I_p^{\alpha} \times B_t^{\beta}$... , H-mode power threshold, number of analyzed shots for the various conditions. ELMy cases: $\dot{W} = 0$. H case: $0.25 \leq \dot{W} \leq 0.33$. * in A_i column: only H^o->D^+ was studied.*

	const	Ip (kA)	Bt (T)	$\bar{n}_e$ (10^3 cm^{-3})	Ptot (MW)	A_I	# data	Pthr (MW)
DV-I st.st.	0.82	0.71 ±0.06		0.18 ±0.05	-0.29 ±0.05	*	150	1.1
DV-I open H	2.04	0.45 ±0.1	0.3 ±0.11	0.2 ±0.09	-0.6 ±0.14	0.46 ±0.21	75	1.8
DV-II closed H bor	0.67	0.68 ±0.05		0.36 ±0.07	-0.49 ±0.09	0.27 ±0.08	217	1.3
DV-II closed H* bor	0.16	1.08 ±0.05			-0.68 ±0.14	0.59 0.07	60	1.4

Recycling aspects were studied for two divertor chamber configurations (divertor chambers DVI / DVII with large / small volumes [9]) and for various stages of "leakiness" of DVII to the main chamber (bypass conductance larger or smaller than the divertor neck conductance). The wall material was either the original stainless-steel wall or carbon or boron layers deposited on it [10]. Table 1 gives the results of τ_E regression analysis (from β_{dia}) and the H-mode power threshold for the various conditions. The divertor configuration affects the parameter scaling of τ_E. Other studies indicated that also the quiescent H-phase has lower confinement in the "leaky" divertor and that carbonization leads to lower confinement quality.

The distribution of the confinement enhancement factor f_H of τ_E with respect to the ITER89-P L-mode scaling is plotted in Fig. 1 for the various conditions considered. The results demonstrate the necessity of having a closed divertor and the advantage of low-Z metallic wall coating. The best confinement is achieved under quiescent conditions with D^o -> D^+ injection, boronization and DVII - closed. f_H is ≈ 2.8.

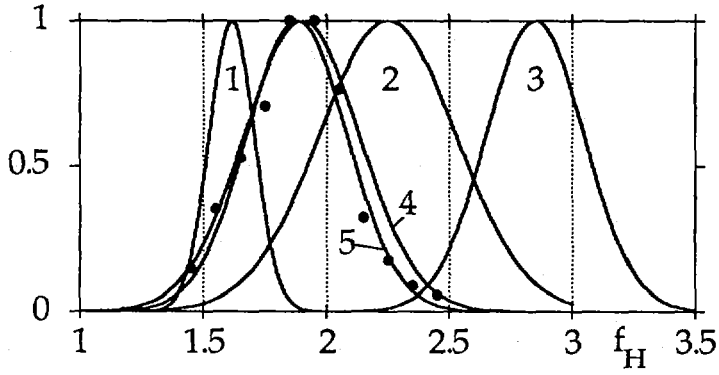

Fig. 1. Distribution of f_H, the ratio of the measured τ_E with that from the ITER 89-P L-mode scaling. 1) DV II " leaky ", 2) DV I stainless-steel walls, closed, 3) DV II H, boronized walls, D^o -> D^+, 4) DV II ELMy, boronized walls, analyzed at β_{MAX}, 5) DV II ELMy, boronized walls, long pulses ($\Delta t > 20\ \tau_E$).*

3 LONG QUASI-STEADY-STATE H-MODES

Attempts to obtain the quiescent H-mode (H*) under steady state conditions on ASDEX were unsuccessful. In addition to the different divertor configurations and wall conditions we tried to develop it under stationary conditions with pumping or non-pumping target plate material (Ti or Cu) and with Ti gettering within the divertor chambers. The longest quiescent H-phases were obtained with boronized walls (duration $\leq$ 220 ms).

Quasi-steady state H-discharges with ELMs require an optimized and constant ELM frequency as is obtained after boronization [11]. The optimum ELM frequency (as a trade-off between impurity level and confinement degradation) is obtained by careful radial and vertical positioning of the plasma column. A movement of 0.5 cm in the vertical direction and 1 cm in the horizontal direction decides between H and H*. A long quasi-steady state H-phase of 3.5 s ($\widehat{=}$ 80 confinement times) is depicted in Figure 2. τ_E = 44 ms; τ_E/I_p = 0.16 s / MA; f_H = 1.9; β / β_{Troyon} = 0.7; ELM period $\approx$ 5.5 ms. Experimental traces are selected which demonstrate steady state conditions for confinement, recycling, and impurities. The longest H-phase (with beam faults, however) was 4.3 s. Figure 1 also shows f_H obtained under ELMy conditions with boronized walls. Two cases are plotted: (1) The usual case with analysis at β_{MAX}; (2) a subset of long quasi-steady state H - phases (> 20 x τ_E) were selected. In order to assess the confinement quality during the pulse, data at 3 moments

are taken: at the beginning, in the middle and at the end of the H-phase: f_H = 1.9. To achieve steady state conditions, a degradation of f_H has to be accepted. A specific study showed that a degradation of 20 % can provide quasi - steady state.

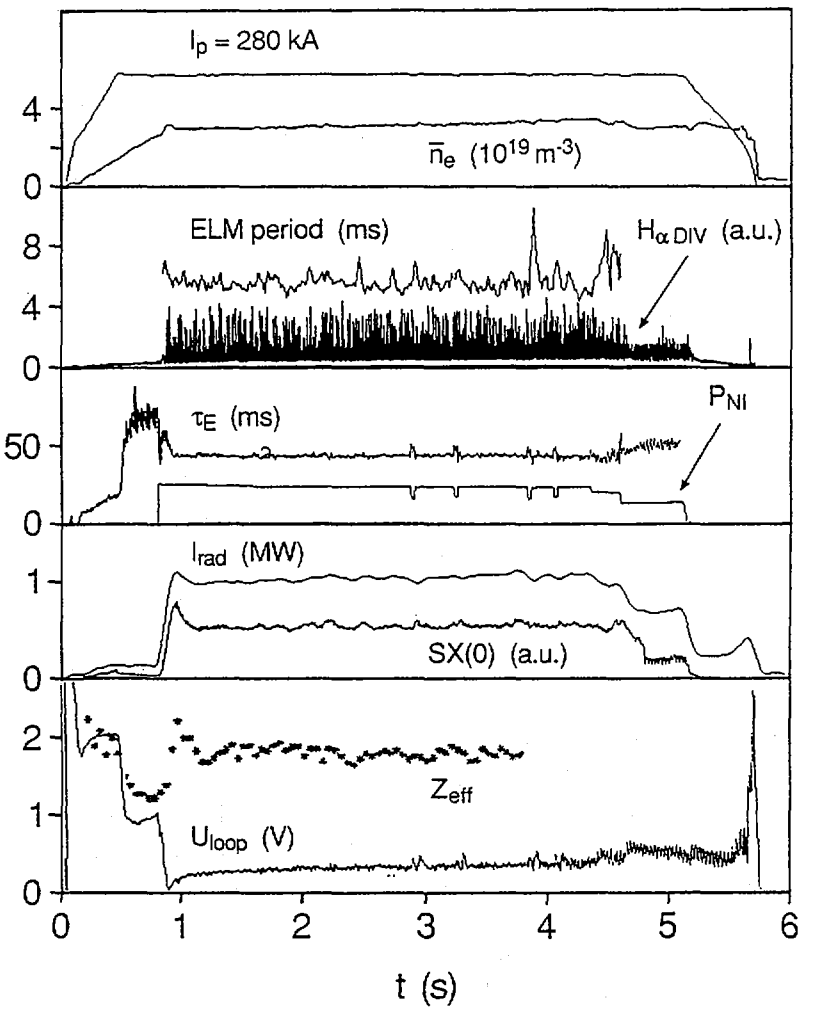

Fig. 2. Example of a quasi-steady state H - discharge. Symbols are standard; Z_{eff} is from Bremsstrahlung; P_{tot} = 1.65 MW.

4 EXPLORATION OF THE H-MODE IN CORNERS OF THE OPERATIONAL WINDOW

4.1. Low-q operation

With boronized walls ELM-free and ELMy H-modes have been studied over a large operational domain: 220 kA $\leq I_p \leq$ 460 kA, 1.25 T $\leq B_t \leq$ 2.8 T, $2.2 \leq q_a \leq 4.5$ [12]. The best fully developed ELM-free H-phases are obtained at values of $q_a \approx 3$. For q_a higher than 3.3 the ELMs are frequent. For $q_a <$ 2.4 the ELM-free phase is interrupted by a hard disruption and the plasma energy cannot reach the values obtained for $q_a > 2.5$. The power threshold to obtain ELM-free H-mode is somewhat higher than for ELMy H-discharges.

The confinement analysis of the ELM-free discharges is performed when β_{pol} is still rising, when the dW/dt correction is 25% - 33% of the total heating power and the radiated power is small. The low q_a discharges - terminated by disruptions - are included. For $P_{tot} >$ 2MW the quality factor τ_E / I_p without ELMs and $D^o \rightarrow D^+ \approx 0.24$ s / MA, for $H^o \rightarrow D^+$ it is $\approx$ 0.20; with ELMs it is 0.14 for hydrogen injection. τ_E / I_p is almost independent of I_p and B_t. In particular, operation at low q_a and high current does not show any pronounced degradation.

4.2. β-limit studies with and without ELMs

A Troyon factor of 2.8 (based on β_{dia}) is obtained both for quiescent H-phases and the phases with ELMs [13]. β-limit operation with ELMs requires, however, a higher heating power.

4.3. Density limit in the H-mode

No detailed density limit program has been carried out. However, at low q_a where the density limit for OH and L-mode plasmas is highest the H-mode density limit has been determined for the H-mode with ELMs. It is comparable to the corresponding L-mode limit. $\bar{n}_e = 1.05 \times 10\,cm^{-3}$ has been obtained corresponding to a Murakami parameter of $10 \times 10^{19} m^{-2} T^{-1}$. f_H at the density limit is 1.85. With pellet refuelling of H-mode discharges values of M up to 13 could be achieved. Owing to the superior particle confinement successful density built up with pellets is possible in the H-mode.

5 POLOIDAL ROTATION

The poloidal rotation of He, C, and B impurities has been measured at the plasma periphery [14]. The measurement on helium-like boron were the

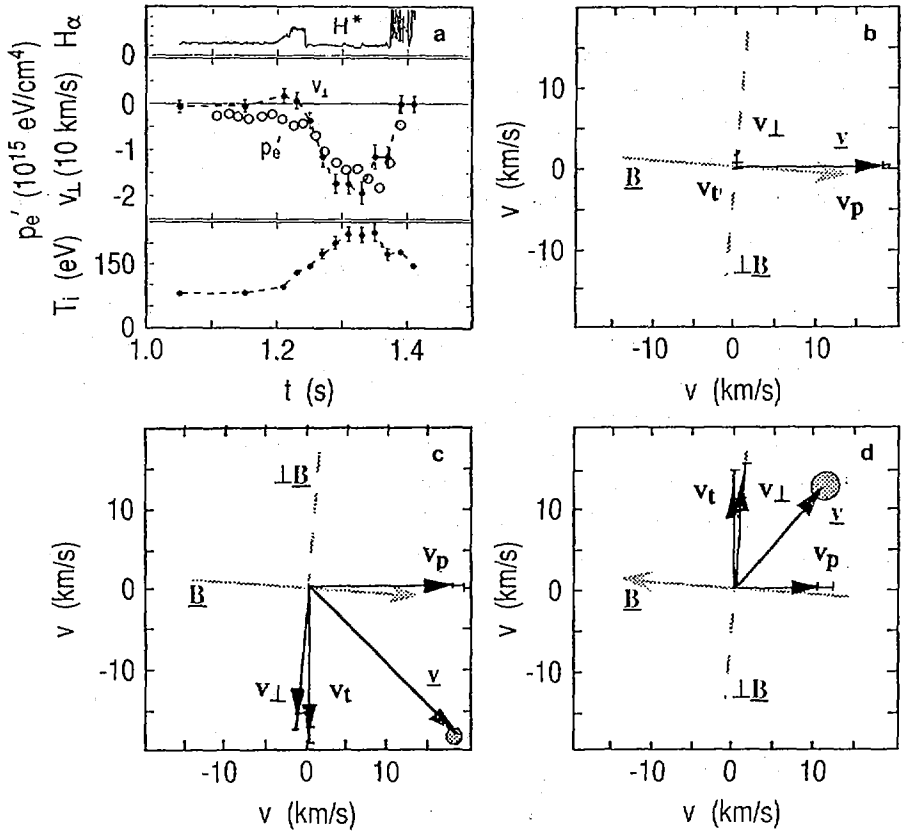

Fig. 3. Poloidal (v_p), perpendicular ($v_\perp$), and toroidal (v_t) drift velocity at the edge. (a) H_α within divertor, time dependence of perpendicular velocity , ion temperature and electron pressure gradient within the thermal barrier, the three velocity vectors in the L-phase (b) and in H^*-modes with different B_t-directions (c,d).

most successful. This impurity developed intrinsically after boronization of the vessel wall. The plasma edge was explored from 36 to 40 cm (a = 40 cm). The measurements were carried out with a scannable mirror system which allows the determination of poloidal (v_p), perpendicular ($v_\perp$), and toroidal (v_t) velocities. The poloidal and perpendicular velocities, given below, are averages from data obtained from opposing viewing directions.

Velocity vectors, as measured in the three directions, are plotted in Fig. 3 for L and two quiescent H-phases with different toroidal field

directions. (For technical reasons, I_p had to be changed with B_t; the negative B_t case is therefore studied in a quiescent H-phase with ctr-NI.) v_t is basically identical for the three cases. (At smaller radii, v_t is larger in the H- than in the L-phase.) In the L-mode v_p and $v_\perp$ are small and point into the direction of $B \times \nabla p$; in the two H - phases v_p and $v_\perp$ are large and point in the $-B \times \nabla p$ (electron drift) direction. v_p and $v_\perp$ change sign when the direction of B_t is changed.

The high poloidal velocity cannot be explained in terms of the pressure gradient of the impurity ion under study but indicates the existence of a strong inward directed radial E-field (confirming the finding of DIII-D [15]) of $|E_r| \leq 20$ kV/m. The gradient in v_p is small; the diagnostic accuracy did not allow for the determination of a gradient in E_r.

v_p and $v_\perp$ increase gradually after the transition and show a temporal variation similar to that of edge gradients. As an example, the edge ion temperature (from Doppler measurements) and p_e' are plotted in Fig. 3. When ELMs occur or in ELMy H-phases v_p and $v_\perp$ decrease and remain at

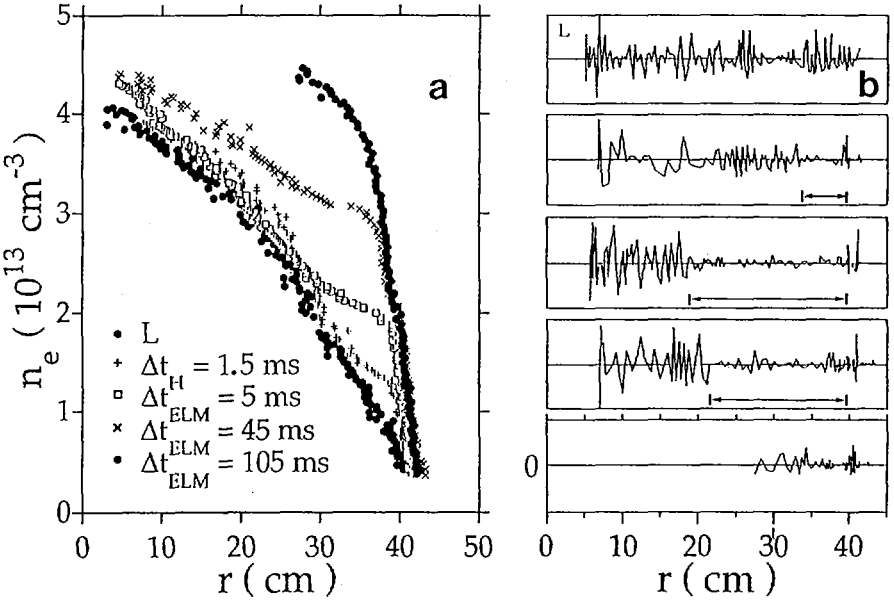

Fig. 4. (a) Development of edge density (reflectometry) from the L-phase, 0.5 ms after the transition and then in a quiescent phase which developed after an ELMy phase; (b) radial variation of edge fluctuations from the L-mode during the H phase for the same time points. I_p = 460 kA; B_t = 2.8 T; P_{tot} = 2.0 MW.*

small values. Nevertheless, in this case also, v_p and $v_\perp$ point in $-B \times \nabla p$ direction. The highest values of v_p and $v_\perp$ (reached toward the end of the H* phase) rise with heating power. The edge drift velocities have also been studied at two different B_t values (I_p was also changed to keep q_a constant). No distinct difference has been observed. These various observations indicate that the origin of E_r may be the pressure or temperature gradients at the edge. E_r corresponding to $E_r = \nabla p_i / n_i e$ (∇p_i being the deuterium pressure gradient ; estimated with the assumption that $p_i' \approx p_e'$) is, however, not more than 50% of the measured one. The neo - classical flow velocity $v_p = -$ const. $\times \nabla T_i / e B$ is approximately 30% of the measured one assuming const. = 1. The collisionalities at the edge prior to the transition are typically $\nu_e^* > 5$ and $\nu_i^* > 10$ (as deduced from edge temperature, density and Z_{eff} measurements). Apart from reflectometry (see Fig. 4), however, none of the edge diagnostics on ASDEX can resolve the actual gradients.

6 TRANSITION AND FLUCTUATION STUDIES

ECE radiometer measurements revealed that an H-transition which is triggered by a sawtooth occurs at the arrival of the heat pulse at the edge. Then the edge transport barrier [3] develops. The H_α radiation decreases at various positions (main plasma chamber, upper and lower, inner and outer divertor chamber) simultaneously within $\approx$ 80 μs. In Fig. 4a the development of the edge density profile (as measured by broadband reflectometry [16]) is shown. The first H-mode profile is obtained $\approx$ 1.5 ms after the H - transition. The transport barrier expands radially during the quiescent phase at constant density gradient. The edge fluctuation level decreases. The most striking observation is the rapid reduction of the edge turbulence measured within the transport barrier by FIR laser scattering. Radially propagating modes are investigated. The fluctuation level drops within < 1 ms to a low level comparable with that during the OH phase (despite of strongly increased edge density). Figure 4b shows the fluctuation level as measured with reflectometry and indicates the radial regions of low fluctuation level during the quiescent H-phase.

Although, originally reduced, the edge fluctuations can strongly increase in the course of the quiescent phase to levels even above those of the L-mode. They are detected by edge FIR scattering, reflectometry, edge soft-X ray emission, and edge electron temperature (radiometer). Unlike the broad-band L-mode turbulence, the fluctuation frequency is around 45 kHz

indicating the coherent nature of these fluctuations. They develop after a delay time in the quiescent phase and do not appear between ELMs. The edge T_e is instantly reduced; the high $v_\perp$ or the density built up are not impaired. The reduction of T_e may ultimately cause the transition back into the L-phase. (Other studies indicate that the back-transition is not caused by excessive impurity radiation.)

7 MHD STUDIES ON ELMS

ELMs are important to keep the ASDEX plasma clean and to produce steady state conditions. Furthermore, as described in paper [17] they contribute to the deposition of heat onto the target plates. Their MHD nature has still not been identified. The T_e-inversion point of ELMs is about 4 - 5 cm inside the separatrix: for $r > 36$ cm T_e transiently increases; $r < 35$ cm it decreases. The inversion radius does not change with q_a (in the range $3.1 \leq q_a \leq 4.2$).

The ELM frequency can vary strongly during the H-phase. Figure 5a shows a plasma with a single ELM shortly after the transition followed by a group of 4 ELMS, then 2 singular ELMs and, finally, a sequence of grassy ELMs. Further MHD effects are a sawtooth in the L-phase (1), one which triggers the H-transition (2), a sawtooth in the quiescent H-phase (4) and one amidst the group of 4 ELMs (5). This sequence of MHD effects was studied with an hf-Mirnov loop (digitizing time 300 ns). Figure 5 (1) - (8) shows the development of the frequency spectra as contour plots. The characteristic low-frequency $m \geq 2$ modes accompanying the $m = 1$ sawtooth precursor, ELM-precursors in the frequency range 100 - 200 kHz followed by a strongly turbulent phase with a frequency spectrum reaching up to 300 kHz at the occurrence of ELMs, are shown. The duration of the turbulent phase, which causes the particle and energy losses, is typically 200 μs. Hf-ELM precursor modes may also appear as transient oscillations without causing an ELM in a manner already familiar from $m \geq 1$ fishbones. The growth rate of an ELM precursor is typically 50 μs. The precursor to the first ELM ($f \approx 180$ kHz) in Fig. 5 (3) has the lowest growth rate. Figure 5 c shows the integrated Mirnov signal for the upper ELM in Fig. 5 (5). The successive turbulent phase is averaged and displays the gross plasma movement. Figure 5 b shows the H_α radiation measured with a fast detector in the main chamber. H_α rises simultaneously within 20 μs at all toroidal positions in the main chamber, in the upper and lower divertor and in the inner and outer divertor SOl.

The ELM features do not differ between ELMs occurring at low pressure shortly after the transition, singular ELMs or in grassy ELM phases.

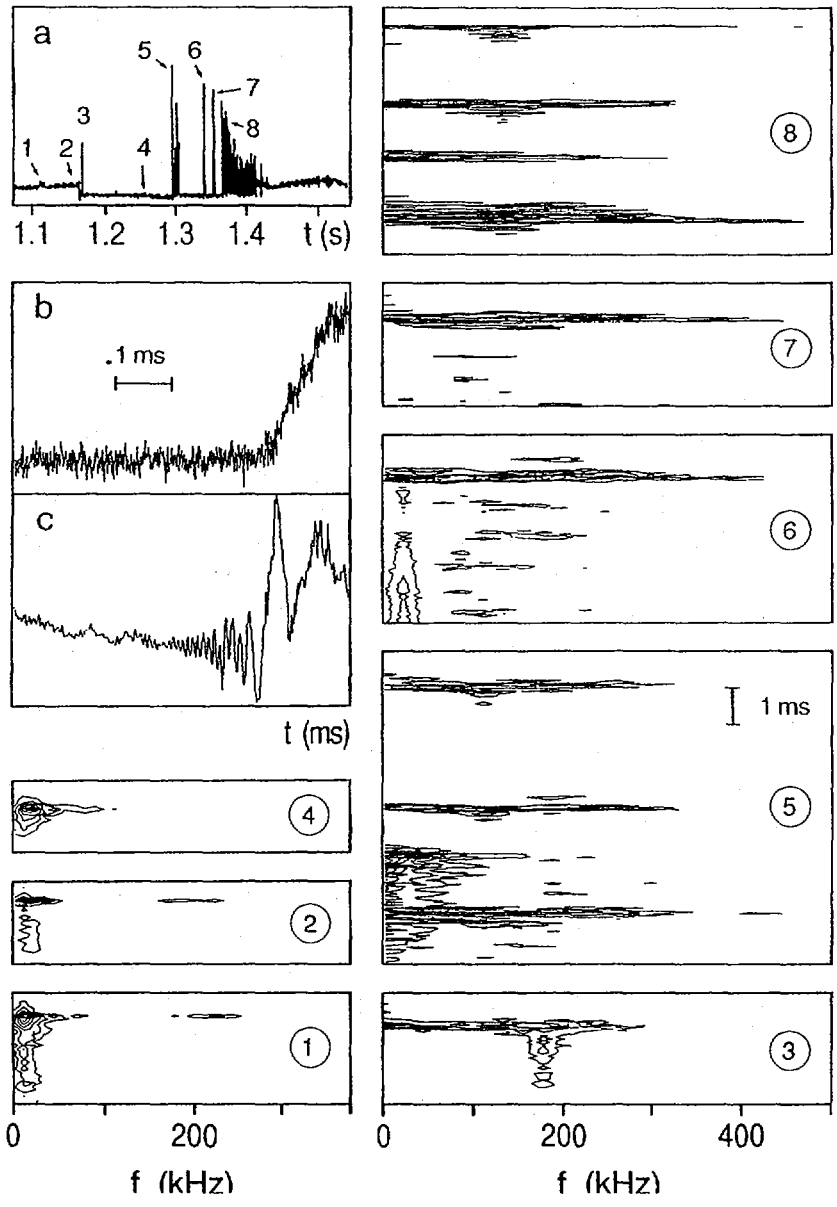

Fig. 5. (a) H_α in the divertor chamber; the numbers indicate the time point of various MHD activity. (b, c) H_α signal in main chamber and Mirnov-loop signal (B_r) of the 3. ELM in (5) . (1) - (8) Time development of frequency spectra for the various MHD effects: (1), (2), (4) sawteeth, (3) - (8) ELMs, (5) 3 ELMs and a sawtooth after the 1st ELM.

The edge electron pressure gradient is stabilized at a lower level by repetitive ELMs . In appropriately positioned discharges (as described above) ELMs can be suppressed and much larger p_e' (scaling with I_p) can be sustained at the edge.

Although we cannot present results on the topology of ELM precursors, the observations are in qualitative agreement with an edge stability analysis presented in Ref. [2].

8 CONCLUSIONS

A comparative study of various confinement regimes revealed the superiority of the H-mode. Although quiescent H-phases do not seem to be suitable for steady-state operation, they might nevertheless be the best scenario for ignition. For continuous burn the transition to the regular H-phase with ELMs might be necessary. Divertor design and wall material seem to be crucial for a large f_H value and for the development of quasi-steady state conditions. For minimizing the ELM-induced losses, the ELM-frequency has to be optimized by proper positioning of the plasma with respect to the vessel. Operation with ELMs does not impair the density - or the β -limit. H-mode operation well below $q_a = 3$ is possible with still good confinement. ELMs are characterized by a precursor in the frequency range of 100 - 200 kHz which initiates a short highly turbulent phase which causes enhanced losses. These features are observed in singular ELMs or in those which appear in a burst of rapid ELMs at low or high edge pressure.

Edge drift velocity measurements indicate the development of a radial E-field close to the separatrix. Whether it corresponds to the bulk ion pressure gradient cannot be resolved. There is, however, indirect evidence: the drift velocity increases gradually during the quiescent H-phase on a time scale similar to that of the edge gradients; both the edge gradients and the drift velocity are strongly reduced in ELMy phases. Edge fluctuations develop in the quiescent H-mode which reduce the edge electron temperature.

REFERENCES

[1] MERTENS, V., et al., in Controlled Fusion and Plasma Physics (Proc. 17th. Eur. Conf. Amsterdam, 1990) to be published in Plasma Phys. Control. Fusion.

[2] ASDEX TEAM, Nucl. Fusion **29** (1989) 1959.

[3] WAGNER, F., et al., Phys. Rev. Lett. **23** (1984) 1453.

[4] KRIEGER, K., et al., in Controlled Fusion and Plasma Physics (Proc. 17th Eur. Conf. Amsterdam, 1990), Vol. 14B, Part III, European Physical Society (1990) 1431.
[5] BESSENRODT-WEBERPALS, M., et al., submitted to Nucl. Fusion.
[6] FUSSMANN, G., et al., in Plasma Physics and Controlled Nuclear Fusion Research 1988 (Proc. 12th Int. Conf. Nice, 1988), Vol. 1, IAEA, Vienna (1989) 145.
[7] WAGNER, F., et al., Nucl. Fusion **25** (1985) 1457.
[8] KAYE, S.M., et al., Nucl. Mater. **121** (1984) 115.
[9] NIEDERMAYER, H., et al., Plasma Phys. Control. Fusion **30** (1988) 1443.
[10] SCHNEIDER, U., et al., J. Nucl. Mater., to be published.
[11] VOLLMER, O., et al., in Controlled Fusion and Plasma Physics (Proc. 17th Eur. Conf. Amsterdam, 1990), Vol. 14B, Part I, European Physical Society (1990) 295.
[12] RYTER, F., et al., ibid., p. 94.
[13] GRUBER, O., et al., in Plasma Physics and Controlled Nuclear Fusion Research 1986 (Proc. 11th Int. Conf. Kyoto, 1986), Vol. 1, IAEA, Vienna (1987) 357.
[14] HOFMANN, J.V., et al., in Controlled Fusion and Plasma Physics (Proc. 17th Eur. Conf. Amsterdam, 1990), Vol. 14B, Part IV, European Physical Society (1990) 1556.
[15] GROEBNER, R.J., et al., Phys. Rev. Lett. **64** (1990) 3015.
[16] MANSO, M.E., et al., 'H-mode Transition Studies with a Novel Reflectometric Technique', IPP Rep. to be published.
[17] NEUHAUSER, J., et al., Paper IAEA-CN-53/A-V-2, these Proceedings, Vol. 1.

DISCUSSION

H. BIGLARI: Since the sampling times of your spectroscopic measurements of poloidal rotation are significantly longer than the time-scale for the L–H transition (< 1 ms), do you think that anything conclusive can really be said on the basis of your data regarding the incidence of (sheared) poloidal flow and the suppression of turbulent fluctuations?

F. WAGNER: About 20% of the overall increase of $v_\perp$ observed during the quiescent H-phase could occur instantly without being detected.

R. R. WEYNANTS: I would like to point out that according to Shaing's theory the electric field has to be about 3–4 times higher after the transition than the pressure gradient term *before* the transition. During the H-mode the electric field can relax to rather close to the pressure gradient term and the plasma will not go out of the H-mode.

K. ITOH: Have you studied the correlation between the frequency and the stationarity of the discharge, for example with regard to impurity content or density? Is there any threshold frequency of ELMs required for a stationary H-mode to be achieved?

F. WAGNER: There is an inverse relation between Z_{eff} and ELM frequency. Our actual task in the experiment was to optimize the conditions in such a way that steady state conditions would prevail at sufficiently low Z_{eff} and sufficiently high confinement time. The example shown had $Z_{eff} < 2$, $f_H \sim 1.9$ and $\beta/\beta_{crit} \sim 0.7$.

R.J. TAYLOR: We are getting closer to agreement with you. What is your spatial resolution on the rotation measurements?

F. WAGNER: About 1 cm.

R.J. TAYLOR: Then I think we are in 100% agreement, and that you have a bifurcated rotation just like those on DIII-D and CCT.